Resonances and Off–Shell Characteristics of Effective Interactions *

S.E. Massen[†a], S.A. Sofianos [a], S.A. Rakityansky [a], S. Oryu [b]

[a] Physics Department, University of South Africa,
P.O.Box 392, Pretoria 0003, South Africa
[b] Department of Physics, Science University of Tokyo,
2641 Yamazaki, Noda, Chiba 278-8510, Japan

February 9, 2008

Abstract

The importance of including experimental resonances in constructing effective inter–cluster interactions has been investigated. For this, we first address the question of how to obtain the analytical properties of the Jost function in regions of physical interest on the complex k–plane when the potential is given in a tabular form. We then employ the Marchenko inverse scattering method to construct, numerically, phase equivalent local potentials supporting the same bound state(s) but having different resonance spectra which affect the off–shell characteristics of the corresponding scattering amplitudes. This implies that the inclusion of the experimental resonances in constructing a potential would change its shape, strength, and range which in turn would modify the bound and scattering wave functions in the interior region. This is expected to have important consequences in calculations of transition amplitudes in nuclear reaction theories, which

*Nuclear Physics A in press

[†]Permanent address: Department of Theoretical Physics, University of Thessaloniki, Thessaloniki 54006, Greece.

strongly depend on the behaviour of the wave functions at short distances. The influence of Supersymmetric Transformations on the position and movement of resonances has also been investigated.

PACS numbers: 03.65.Nk, 12.40.Qq, 21.30.+y, 34.20.-b

1 Introduction

A central problem of the theory of nuclear reactions is to find the interaction potential between the colliding nuclei that can describe a wide range of scattering data and provide the wave functions required. Such a potential is not simply the result of mapping data to a convenient functional form. Rather, it has an underlying physical basis in that it is related to the nucleon–nucleon interaction as well as to the structure and dynamics of the interacting nuclei.

For practical reasons, it is desirable to express this potential in terms of quite simple analytic and local form with parameters adjusted to fit a set of scattering data. The phenomenological optical model potentials [1] are of this class. The most commonly used form is that of a Woods–Saxon shape and for light nuclei that of a Gaussian. As these potentials fit the scattering cross section well, the relevant scattering wave function is asymptotically correct. Such potentials, however, do not guarantee that their off–shell characteristics are sufficiently good to describe equally well reactions that depend on the behaviour of the wave function in the interior region. Such reactions are, for example, the electro–disintegration and photo–disintegration processes which depend crucially on the wave function at all distances.

When a nucleus–nucleus interaction is constructed theoretically directly from a nucleon–nucleon potential, it is usually nonlocal and quite complicated. Such potentials can be obtain, for example, by using the Resonating Group Method (RGM) in which the inter–cluster interaction is constructed via the Pauli antisymmetrization [2]. To study the resulting nonlocalities one resorts to a construction of an equivalent local potential (ELP) using various methods. In this way certain off–shell characteristics of the interaction can be revealed. For instance, the use of Fiedeldey's Wronskian method [3, 4] to construct an energy dependent ELP for the nucleon–α RGM nonlocal interaction revealed a repulsion in the interaction region [5] which suggests the possible existence of resonances.

Another way of constructing local nucleus–nucleus potentials is the use of inverse scattering techniques. The potential in this case is directly related to the available information of the scattering phase shifts and of bound states. In the inverse scattering method at a specific partial wave ℓ (fixed–ℓ inversion) [6, 7, 8] and in the absence of bound states, the constructed potential is unique. However, when bound states are present one may construct an infinite number of potentials which are spectrum and phase equivalent at all energies. This is achieved by choosing arbitrarily the bound states normalization constants which are not available from experiments. However, as we shall show in this paper, the asymptotic normalization constants determine the distribution of resonances in the k–plane and vice versa. This emphasizes the importance of taking resonances into account in constructing effective interactions which are usually ignored.

One of the main reasons for omitting the resonances is the lack of experimental information on their positions and widths especially for broad resonances. In the past this was aggravated by the absence of an exact and yet simple method to study the analytical properties of the corresponding amplitude which could facilitate their incorporation into the potential construction. Recently, however, a new method for direct calculation of the Jost function in the complex k–plane, has been developed [9, 10, 11, 12]. Within this method, the bound, resonant, and scattering states can be found by locating the Jost function zeros in the appropriate domain of the k–plane. It is based on a combination of the complex coordinate rotation with the variable–constant method used to replace the Schrödinger equation by an equivalent system of linear first–order differential equations. Since this method is both exact and quite simple, it could be used, together with the fitting of phase shifts, to construct a realistic potential which reproduces resonance poles as well.

Complex rotation of the coordinate requires knowledge of the potential off the real axis in the r–plane. This poses no problem when the potential is given in an analytic form. However, there are cases, such as the aforementioned inverse scattering method, in which the resulting potential is given as a tabulated set of values versus radial points. In this paper, we show how the Jost function method of Refs. [9, 10, 11, 12] can be extended to deal with such potentials, and then apply it to study the resonances and their effects on the off–shell characteristics of phase equivalent potentials obtained numerically by the Marchenko inversion and in Supersymmetric (SUSY) transformations.

In Sec. II we will describe our formalism by briefly recalling the Marchenko inversion method, the relevant SUSY transformations, and the exact method of obtaining resonances and Regge trajectories. Our results are presented in Sec. III and our conclusions are given in Sec. IV. In the Appendix we present some technical details related to the inverse method and the Jost function.

2 Formalism

2.1 Inverse scattering method

In the Marchenko inversion scheme [6, 7, 8] the potential $V_\ell(r)$, for each partial wave ℓ, is obtained from the relation

$$V_\ell(r) = -2\frac{\mathrm{d}K_\ell(r,r)}{\mathrm{d}r} \tag{1}$$

where the function $K_\ell(r,r')$ satisfies the Marchenko fundamental integral equation

$$K_\ell(r,r') + \mathcal{F}_\ell(r,r') + \int_r^\infty K_\ell(r,s)\mathcal{F}_\ell(s,r')\mathrm{d}s = 0\ . \tag{2}$$

The kernel $\mathcal{F}_\ell(r,r')$ of this equation is related to the S–matrix $S_\ell(k)$, and thus to experiment, via

$$\mathcal{F}_\ell(r,r') = \frac{1}{2\pi}\int_{-\infty}^{\infty} h_\ell^{(+)}(kr)\left[1 - S_\ell(k)\right] h_\ell^{(+)}(kr')\mathrm{d}k - \sum_{n=0}^{N_b-1} A_{n\ell} h_\ell^{(+)}(b_n r) h_\ell^{(+)}(b_n r')\ , \tag{3}$$

where $h_\ell^{(+)}(z)$ is the Riccati–Hankel function, N_b is the number of bound states, and $A_{n\ell}$ is the asymptotic normalization constant [7, 8] for the nth bound state with energy $E_b^{(n)} = -\hbar^2 b_n^2/2\mu$ where ib_n lies on the positive imaginary axis of the k–plane. The $A_{n\ell}$ can be expressed in terms of the relevant Jost solution $\mathrm{f}_\ell^{(+)}(k,r)$

$$A_{n\ell}^{-1} = \int_0^\infty \left[\mathrm{f}_\ell^{(+)}(ib_n, r)\right]^2 \mathrm{d}r\,. \tag{4}$$

The S–matrix needed in Eq. (3) can be parametrized using the convenient rational ansatz,

$$S_\ell(k) = \prod_{i=1}^{\infty} \frac{k + a_i}{k - a_i}\ , \tag{5}$$

i.e. using an infinite number of simple poles and zeros. In practice the number of a_i in the above formula is limited to N which is sufficiently large to reproduce the input scattering phase shifts and bound states. The conventions and a method to evaluate these N constants are described in Appendix A. The rational parametrization of the S–matrix reduces the Marchenko inverse scattering procedure to an algebraic problem since the kernel of Eq. (2) becomes separable; this can easily be seen if one performs the integration in Eq. (3) using the residue method.

In the absence of bound states the above scheme is unique, *i.e.*, once a good fit to the data from $(0, \infty)$ is achieved, one and only one potential can be obtained. In the presence of bound states, however, the potential is not unique as it depends on the choice of the asymptotic normalization constants $A_{n\ell}$ which are not provided by experiment. When $A_{n\ell}$ are chosen according to Eq. (4) or, equivalently, obtained via the Jost function $f_\ell(k)$,

$$A_{n\ell} = \left[i \frac{f_\ell(-k)}{\mathrm{d}f_\ell(k)/\mathrm{d}k} \right]_{k=ib_n} , \tag{6}$$

the resulting potential is unique and has the shorter range [8]. Any other choice can lead to an equivalent local potential which reproduces the same on–shell data but it has different shape and range.

From Eq. (6) it is clear that values of the normalization constants are determined by the explicit form of the Jost function, if known. The $A_{n\ell}$ can be easily obtained using Eq. (6) where the Jost function is parametrized using also a rational representation

$$f_\ell(k) = \prod_{i=1}^{\infty} \frac{k - \alpha_i}{k - \beta_i} . \tag{7}$$

A way to select the alphas and betas, for a finite number of terms used in the parametrization (5) or (7), is described in the Appendix.

The Jost function thus constructed approximates well the exact Jost function on a segment of the real axis of the k–plane. From this one should expect that it would be a good approximation off the real axis as well. Indeed, if two analytical functions coincide on any arc of a continuous curve, they coincide everywhere in the region of their analyticity [13].

There are at least two problems concerning such a parametrization. Firstly, the function (7) actually does not coincide with the exact Jost function on

the real axis but can only be a good numerical approximation at certain points. How fast the deviations are growing when one moves away from the real axis is not known. Secondly, since instead of an infinite number of terms in Eq. (7), we have to truncate the product to a finite number of terms, not all α_i correspond to zeros of the exact Jost function. In other words, the fitting procedure employed to evaluate these parameters, may generates a number of unphysical zeros and poles which could be simply an artifact of the truncation.

2.2 Supersymmetric Transformation

The inter–cluster interaction in nuclear physics is usually characterized by a repulsion at short distances. Alternatively, the potential can be made deep enough to sustain deep bound states which simulate the role of the so-called Pauli Forbidden States (PFS) appearing in the RGM theory which are not physical. This means that the Levinson's theorem, $\delta_0(0) - \delta_0(\infty) = \pi$, is fulfilled for this system. These states, however, pose a problem when the potential is intended for used in few–body calculations as they generate a scattering amplitude with different off–shell characteristics. Thus one resorts to the removal of the PFS using a subtraction technique [14] that results in a shallow potential. A rigorous relation between deep and shallow potentials, however, has been established by Baye [15] by using two successive SUSY transformations, the first in order to remove the ground state and the second to restore phase equivalence. Alternatively the ground state can be removed using the Marchenko inverse scattering method and assigning a zero value to the corresponding asymptotic normalization constant. The resulting potential is also unique [16] coinciding with the one obtained from SUSY transformations. In what follows, the main equations of the supersymmetric transformation will be briefly recalled (details can be found, for example, in Refs. [15, 17]).

The supersymmetric transformation of a given potential $V_\ell^{(0)}$ that has an undesirable ground state at $E = E_b^{(0)} = -\hbar^2 b_0^2/2\mu$, results in a phase–equivalent potential $V_\ell^{(2)}$ which does not sustain this state. Two consecutive transformations,

$$V_\ell^{(0)} \Longrightarrow V_\ell^{(1)} \Longrightarrow V_\ell^{(2)} \ , \tag{8}$$

are required for this purpose. The first one eliminates the ground state of

the original potential, but also changes the phase shifts. Phase equivalence is then restored by a second SUSY transformation. The first step of the transformation (8),

$$V_\ell^{(1)}(r) = V_\ell^{(0)}(r) - 2\frac{\mathrm{d}^2}{\mathrm{d}r^2} \ln \Psi_{0\ell}^{(0)}(ib_0, r) \ , \tag{9}$$

requires the normalized wave function $\Psi_{0\ell}^{(0)}(ib_0, r)$ of the ground state to be removed. The second step is implemented via

$$V_\ell^{(2)}(r) = V_\ell^{(0)}(r) - 2\frac{\mathrm{d}^2}{\mathrm{d}r^2} \ln \left[\Psi_{0\ell}^{(0)}(ib_0, r)\Psi_\ell^{(1)}(ib_0, r)\right] \ , \tag{10}$$

where the wave function $\Psi_\ell^{(1)}(ib_0, r)$ is the solution of the Schrödinger equation with the potential $V_\ell^{(1)}(r)$ at the same energy $E = E_b^{(0)}$ and has the asymptotic behaviour

$$\Psi_\ell^{(1)}(ib_0, r) \underset{r\to\infty}{\longrightarrow} \exp(b_0 r) \ .$$

The well–known $1/r^2$ behaviour of the transformed potential $V_\ell^{(2)}(r)$ at short distances can easily be deduced from Eq. (10). Indeed, both wave functions $\Psi_{0\ell}^{(0)}(ib_0, r)$ and $\Psi_\ell^{(1)}(ib_0, r)$ near the origin have the behaviour $\sim r^m$ with some integer m, which makes the second term of this equation proportional to $\sim 1/r^2$.

Finally, we note that the SUSY potentials are intrinsically related to inverse scattering theory [17] which can be used to generate energy–independent shallow potentials from energy–dependent deep potentials [18]. For this, one has to calculate first the phase shifts at all energies and then employ the Marchenko scheme to construct an ℓ–dependent potential from which a unique shallow potential can be obtained either by super transforming twice or, as mentioned earlier, by assuming that the corresponding asymptotic normalization constant is zero.

2.3 Exact method for locating resonances

The method we employ here for locating potential resonances belongs to the class of so-called complex energy methods which are based on a rigorous definition of resonances, namely, as zeros of the Jost function. Unlike most

of the other methods of this class, which involve an expansion of the resonant wave function in terms of square–integrable functions, our method is based on a direct calculation of the Jost function at complex k by integrating exact differential equations equivalent to the Schrödinger equation.

By locating a complex zero k_r of the Jost function in the fourth quadrant of the momentum plane, we can obtain, at the same time, the resonant energy E_r and width Γ from the simple relation

$$E_r - \frac{i}{2}\Gamma = \frac{\hbar^2}{2\mu}k_r^2 \ .$$

It is clear that the accuracy of E_r and Γ is related to the accuracy in calculating the Jost function itself. The latter is obtained, in our method, from the asymptotic value of a function $F_\ell^{(-)}(k,r)$,

$$f_\ell(k) = \lim_{|r|\to\infty} F_\ell^{(-)}(k,r) \ , \tag{11}$$

which, together with its partner $F_\ell^{(+)}(k,r)$, obeys the system of first order differential equations

$$\partial_r F_\ell^{(+)}(k,r) = \frac{h_\ell^{(-)}(kr)}{2ik} V_\ell(r) \left[h_\ell^{(+)}(kr) F_\ell^{(+)}(k,r) + h_\ell^{(-)}(kr) F_\ell^{(-)}(k,r) \right] \ , \tag{12}$$

$$\partial_r F_\ell^{(-)}(k,r) = -\frac{h_\ell^{(+)}(kr)}{2ik} V_\ell(r) \left[h_\ell^{(+)}(kr) F_\ell^{(+)}(k,r) + h_\ell^{(-)}(kr) F_\ell^{(-)}(k,r) \right]$$

the boundary conditions being

$$F_\ell^{(\pm)}(k,0) = 1 \ . \tag{13}$$

The origin of the relation (11) becomes clear if one notices that the sum of the products of the auxiliary functions $F_\ell^{(\pm)}(k,r)$ with the Riccati–Hankel functions,

$$\phi_\ell(k,r) = \frac{1}{2}\left[h_\ell^{(+)}(kr) F_\ell^{(+)}(k,r) + h_\ell^{(-)}(kr) F_\ell^{(-)}(k,r) \right] \ , \tag{14}$$

obeys the Schrödinger equation. The function $\phi_\ell(k,r)$ is the so-called *regular solution* which vanishes near $r = 0$ exactly like the Riccati–Bessel function, *i.e.*

$$\lim_{r\to 0} \phi_\ell(k,r)/j_\ell(kr) = 1 \ . \tag{15}$$

The Jost function, Eq. (11), can be obtained by comparing the asymptotic behaviour of the regular solution,

$$\phi_\ell(k,r) = \underset{r\to\infty}{\longrightarrow} \frac{1}{2}\left[h_\ell^{(+)}(kr) f_\ell^*(k^*) + h_\ell^{(-)}(kr) f_\ell(k)\right] \ , \tag{16}$$

with Eq. (14) expressed in terms of the auxiliary functions $F_\ell^{(\pm)}(k,r)$.

In Ref. [10] it has been shown that the limit (11) exists for all complex k for which

$$\mathrm{Im}\, kr \geq 0 \ . \tag{17}$$

If r is real, the condition (17) is only satisfied for bound and scattering states but not for resonances. Therefore, to calculate $f_\ell(k)$ in the fourth quadrant we make the complex rotation of the coordinate in Eqs. (12),

$$r = x\exp(i\theta)\,, \qquad x \geq 0\,, \qquad 0 \leq \theta < \frac{\pi}{2}\ , \tag{18}$$

with a sufficiently large θ.

The above scheme works extremely well in locating bound, scattering, and resonant states as well in finding Regge poles and trajectories when the potential $V_\ell(r)$ is central, short range and it is given in analytic form. A generalization to non–central, multi–channel, and Coulomb–tailed as well as to singular potentials can be found in Refs. [9, 10, 11, 12]. However, in this work we are concerned with potentials given in a tabular form and the question of how to handle such potentials will be discussed when presenting our results.

3 Results

In the present work the potentials were generated either by inversion or by SUSY transformations and hence in both cases they are available in a tabular form. To make an analytic continuation of them into the first quadrant of the complex r–plane, needed for the complex rotation, we fitted the potentials on the real axis by simple analytical forms with adjustable parameters and then considered r in these forms as a complex variable. Such an approach to analytic continuation is based on a theorem of the complex analysis which states that if a function is analytic in a region and vanishes along any arc of a continuous curve in this region, then it must vanish identically in this region

[13]. The obvious corollary of this theorem is that if two functions coincide on a curve, they coincide everywhere in the region of analyticity. Therefore, the analytical form which coincides with the tabulated function on the real axis should reproduce this function off the real axis as well. The question then arises what if the potentials coincide within numerics. In other words, we want to know whether small numerical deviations in the potential on the real axis generate perceptible deviations of the position of the resonances. We have investigated this situation first by assuming the following analytic potential

$$V(r) = 5\exp\left[-0.25(r-3.5)^2\right] - 8\exp(-0.2r^2) \tag{19}$$

where the strength parameters are given in MeV and r in fm. The reduced mass μ is such that $\hbar^2/2\mu = 1/2\,\mathrm{MeV\,fm}^2$. The resonances and Regge trajectories of this potential were investigated in Ref. [10]. We then fitted the N points $V(r_i)$, $i = 1, 2, \cdots, N$ using the ansatz

$$V_{\rm fit}(r) = \sum_{n=1}^{N_1} a_n \exp\left[-b_n(r-c_n)^2\right] + \sum_{n=1}^{N_2} d_n \exp(-e_n r^2) \tag{20}$$

where the parameters were obtained using the MERLIN minimization program [19]. The minimization was stopped when the least square error on 120 points and $N_1 = 5$ and $N_2 = 4$ was of the order of 10^{-4} – a typical accuracy in these cases. This means that the fit to the analytic potential was between the third and fourth decimal in the whole region. With such a fit, all resonances found in Ref. [10] were recovered within three to five decimal points. For comparison, the energies and widths for few of them (the lowest resonances in each partial wave) are given in Table 1. Obviously the accuracy can be improved as the fit to the potential improves. One further comment is necessary: The form factors used for the fit restrict the use of a rotation to only a certain region. In this respect the use of splines is not suitable at all as they diverge for all angles of rotation.

These test calculations show that the Jost function method based on the complex rotation of the coordinate, is applicable and retains its effectiveness even when the potential is given numerically on the real axis. We can therefore use it to study the importance of incorporating physical two–cluster resonances in constructing a potential. This can be easily investigated by constructing ELP's for a specific partial wave via inversion as described above and studying the implications of the implanted resonances. For this we

use the nucleon–α potential of Dubovichenko and Dzhazairov–Kakhramanov [20] for the $\ell = 0$ partial wave

$$V(r) = -V_0 \exp(-\alpha r^2) \tag{21}$$

where $V_0 = 55.774\,\mathrm{MeV}$ and $\alpha = 0.292\,\mathrm{fm}^{-2}$. This is a deep potential that sustains an unphysical PFS state at $-9.73058\,\mathrm{MeV}$. This means that the Levinson's theorem, $\delta_0(0) - \delta_0(\infty) = \pi$, is fulfilled for this system. At large distances the radial wave function decays exponentially,

$$u_0(r) \underset{r\to\infty}{\longrightarrow} A_s \exp(-b_0 r) \ ,$$

and the asymptotic normalization constant was found to be $A_s = 6.1603\,\mathrm{fm}^{-1/2}$.

By varying the asymptotic normalization constant we obtained a set of potentials which were fully phase shift and bound state equivalent but have different number of potential resonances. These potentials are shown in Fig. 1. It is seen that for values of A_s less than the choice given by (4) ($A_s = 6.1603$), a hump appears in the interaction region which is higher as A_s becomes smaller while at the same time the well becomes deeper. For values larger than 6.1603 the potential is also of long range but without a hump. In the extreme case of $A_s = 0$ the potential becomes repulsive at all distances. This means that as $A_s \to 0$ resonances are generated and their appearance and position depend on the specific choice of A_s.

Using the ansatz (20) we fitted these potentials, with $N_1 = 5$ and $N_2 = 3$, via the MERLIN code [19] the accuracy being again within a fourth decimal at all points meaning that corresponding accuracy in reproducing the phase shifts was better than 0.0001 of a degree. We employed the analytical representations of these phase–equivalent potentials to locate the zeros of the Jost function in the fourth quadrant of the k–plane. The original potential (21), which is also a member of our set of the phase–equivalent potentials, does not generate any physical resonances. All the zeros of the Jost function, which we found for this potential, are situated below the diagonal of the fourth quadrant of the k–plane and, therefore, represent sub–threshold resonances which are unphysical. The growth of the potential barrier when A_s decreases, indicates that some physical resonances should appear. In other words, when A_s becomes smaller some of the Jost function zeros should move up to the area above the threshold line. When, however, A_s is too small, the barrier transforms into a strong repulsive core, and the resonances should

disappear. This can be seen in Fig. 2 where we present the distributions of the Jost function zeros for three phase–equivalent potentials corresponding to A_s equal to 3, 2 and 1. It is clear that the choice of A_s determines positions of the resonances and vice versa.

At a first sight one can argue that the zeros of the Jost function practically have no effect on the scattering processes because they are far away from the real axis. These potentials, however, generate bound and scattering wave functions which have a different behaviour in the interior region. The bound state wave functions are shown in Fig. 3 while the scattering wave functions, for center of mass energy $E = 5\,\mathrm{MeV}$, are plotted in Fig. 4. The nodeless wave function for the SUSY potential $V^{(2)}(r)$ is also shown in the latter. Since the interior region (within few fm) is of importance in describing various nuclear reactions, the existence and distribution of resonances cannot be ignored when the reaction observables are calculated. These differences are also a source of off shell differences in the corresponding scattering matrices which are manifested in three– and four–cluster calculations.

As another example, we consider the α–α local potential of Buck *et al.* [21]

$$V(r) = -V_0 \exp(-\alpha r^2) + \frac{4e^2}{r}\mathrm{erf}(\beta r)\ , \tag{22}$$

with $V_0 = 122.6225\,\mathrm{MeV}$, $\alpha = 0.22\,\mathrm{fm}^{-2}$, and $\beta = 0.75\,\mathrm{fm}^{-1}$. This potential sustains, in the $\ell = 0$ partial wave, two unphysical deep bound states at $-72.78\,\mathrm{MeV}$ and $-22.28\,\mathrm{MeV}$ and a resonance at $179.22\,\mathrm{keV}$ with $\Gamma = 0.94905\,\mathrm{keV}$. The position of the resonance is quite different from the values of $92.12\pm0.05\,\mathrm{keV}$ and $\Gamma = 5.80\,\mathrm{eV}$ given by Buck *et al.* [21]). A possible reason for such a discrepancy is that in locating these spectral points we included the Coulomb tail of the second term of Eq. (22) in an exact way as was proposed in Refs. [9, 10]. We are interested about the movement of this resonance when we eliminate one of the unphysical bound states using the SUSY transformation. To this end, the numerically obtained SUSY potential $V^{(2)}$ was fitted using the ansatz

$$V_{\mathrm{fit}}(r) = \sum_{n=1}^{5} a_n \exp(-b_n r^2)/r^2 + \sum_{n=1}^{5} c_n \exp(-c_n r^2) \tag{23}$$

with the accuracy of the fit of 450 points being better than 10^{-5}. Using this analytic potential, we found a zero of the S–wave Jost function at $k =$

$0.10383 - i0.77289 \times 10^{-5}\,\mathrm{fm}^{-1}$ (*i.e.* at $E = 0.11261 - \frac{i}{2}0.33532 \times 10^{-4}\,\mathrm{MeV}$) which is significantly different from the position of the S–wave resonance given in Table 2. In view of the above discussion this is not surprising since the SUSY transformation drastically changes the asymptotic normalization constant for the ground state, to zero.

4 Conclusion

We demonstrated that for a potential given numerically the analytic properties of the corresponding Jost function in the complex k–plane can be obtained via fitting the potential by any analytic form that allows a complex rotation into the first quadrant of the complex r–plane. The scattering observables, the bound states, and the potential resonances can be calculated with a sufficient accuracy which is improved with an improved fit to the potential.

The phase shifts and therefore the on-shell S–matrix which are extracted from experimental data on the real k–axis, contain information about resonances in an indirect way. The phase-shifts "feel" the existence of resonances only when they are close to the real axis (narrow resonances). The broad resonances, however, remain "unnoticed" by the phase-shifts and therefore a potential which is based on them, generates an S–matrix without the corresponding poles. However, even extremely broad resonances affect the behaviour of the physical wave function at short distances. This implies that an information on the distribution of resonances can be a clue for making a correct choice among very different potentials generating the same phase-shifts and the same on-shell S–matrix.

Such information can, in principle, be obtained from various inelastic processes. For example, photo-excitation of a nucleus and its subsequent decay in two fragments A and B can reveal AB–resonances which are not "visible" in elastic AB–scattering. When an effective potential is constructed using not experimental but theoretical phase–shifts, additional effort to locate broad resonances would exclude ambiguities (non-uniqueness) of the effective potential. This is the case, for example, with the RGM theory which can produce very complicated (nonlocal) potentials. To apply such a potential in realistic calculations, one usually calculates RGM phase-shifts and, using them, constructs a simple effective (phase-equivalent) potential.

In summary, when constructing a realistic effective interaction, it is important to take into account physical resonances. In the case of an energy– and ℓ–independent potential, the resonances at all partial wave must be incorporated. This will guarantee that a reliable local potential is obtained that generates a transition matrix which has correct off–shell behaviour.

acknowledgements

We gratefully acknowledge financial support from the Foundation for Research Development of South Africa and the Science University of Tokyo. Useful discussions with P.E. Hodgson are also acknowledged.

References

[1] P.E. Hodgson, *The Nucleon Optical Potential*, (World Scientific, 1994).

[2] K. Wildermuth and Y. C. Tang, *A unified theory of the Nucleus*, in *Clustering Phenomena of the Nucleus* Vol. 1, (Brounsceving, Viliveg, 1977).

[3] H. Fiedeldey, Nucl. Phys. **77**, 149 (1966).

[4] H. Fiedeldey and S. A. Sofianos, Z. Phys, **A311**, 339 (1983).

[5] S. A. Sofianos, Phys. Rev. C**35**, 894 (1987).

[6] Z. S. Agranovich and V. A. Marchenko, *The Inverse Problem of Scattering Theory*, (Gordon & Breach, New York), 1964

[7] K. Chadan and P. C. Sabatier *Inverse Problems in Quantum Scattering Theory*, (Springer, New York), 1989.

[8] R. G. Newton, *Scattering Theory of Waves and Particle*, 2nd ed. (Springer, New York, 1982).

[9] S. A. Rakityansky, S. A. Sofianos, and K. Amos, Il Nuovo Cim. B **111**, 363 (1996).

[10] S. A. Sofianos and S. A. Rakityansky, J. Phys. A: Math. Gen. **30**, 3725 (1997).

[11] S. A. Rakityansky and S. A. Sofianos, J. Phys. A: Math. Gen, **31**, 5149 (1998).

[12] S. A. Sofianos, S. A. Rakityansky, and S. E. Massen, to appear in Phys. Rev. A (1999), available from the Los Alamos e-print archive as **nucl-th/9901023**.

[13] P. M. Morse and H. Feshbach, *Methods of theoretical physics*, (McGrow-Hill Book Company, New York, 1953) p. 390.

[14] V. I. Kukulin, V. N. Pomerantsev, A. Faessler, A. J. Buchmann, E. M. Tursunov, Phys. Rev. C **57**, 535 (1998).

[15] D. Baye, Phys. Rev. Lett. **58**, 2738 (1987); J. Phys. A **20**, 5529 (1987).

[16] S. A. Sofianos, A. Papastylianos, H. Fiedeldy, and E. O. Alt, Phys. Rev. C **42**, R506, (1990).

[17] C. V. Sukumar, J. Phys. A **18**, L57 (1985); J. Phys. A **18**, 2937 (1985); J. Phys. A **18**, **18**, 2937 (1985).

[18] H. Fiedeldy, S. A. Sofianos, A. Papastylianos K. Amos, and L. J. Allen, Phys. Rev. C **42**, 411, (1990).

[19] D. G. Papageorgiou, I. N. Demetropoulos, and I. E. Lagaris, Comp. Phys. Comm., **109**, 227 (1998).

[20] S. B. Dubovichenko and A. V. Dzhazairov-Kakhramanov, Sov. J. Nucl. Phys. **51**971 (1990).

[21] B. Buck, H. Friedrich, and C. Wheatley, Nucl. Phys. **A275**, 246 (1977).

A Distribution of the S–function poles in the complex k–plane

The S–function is defined in terms of the Jost functions by

$$S_\ell(k) = \frac{f_\ell^*(k^*)}{f_\ell(k)} \tag{24}$$

The $f_\ell(k)$ can be parametrized using the rational form

$$f_\ell(k) = \prod_{i=1}^{N} \frac{k-\alpha_i}{k-\beta_i} \tag{25}$$

implying that it has N simple poles at $k=\beta_i$ and N simple zeros at $k=\alpha_i$. The $f(k)$ is a well defined function in the upper-half k–plane. The poles β_i are therefore situated in the lower k–plane. In contrast, the α_i can be in both planes. Those in the upper half k–plane are denoted by τ_i and those in the lower by σ_i. For the S_ℓ–function we have

$$S_\ell(k) = \prod_{i=1}^{N} \frac{k+\alpha_i}{k-\alpha_i}\frac{k-\beta_i}{k+\beta_i} \tag{26}$$

or

$$S_\ell(k) = \prod_{m=1}^{N_\sigma} \frac{k+\sigma_m}{k-\sigma_m} \prod_{n=1}^{N_\tau} \frac{k+\tau_n}{k-\tau_n} \prod_{i=1}^{N} \frac{k-\beta_i}{k+\beta_i}\,, \quad N_\sigma + N_\tau = N \tag{27}$$

Setting $\xi_i = -\beta_i$ ($\mathrm{Im}\,\xi_i > 0$) we may rewrite Eq. (27) as

$$S_\ell(k) = \prod_{m=1}^{N_\sigma} \frac{k+\sigma_m}{k-\sigma_m} \prod_{n=1}^{N_\tau} \frac{k+\tau_n}{k-\tau_n} \prod_{i=1}^{N_\xi} \frac{k+\xi_i}{k-\xi_i} \tag{28}$$

or adopting the same symbols for all poles and roots

$$S_\ell(k) = \prod_{m=1}^{M} \frac{k+a_m}{k-a_m}\,, \qquad M = 2N \tag{29}$$

It is clear that the number of poles N_ξ, N_σ, and N_τ for the ξ, σ, and τ poles are related by $N_\xi = N_\sigma + N_\tau$.

The form (29) is the one used to parametrized the S–function or equivalently the phase-shifts δ. This can be easily achieved by rewriting (29) in the form

$$S_\ell(k) = \frac{1 + \sum_{m=1}^{M} A_m k^m}{1 + \sum_{m=1}^{M} (-1)^m A_m k^m} \tag{30}$$

or

$$S_\ell(k) + S_\ell(k) \sum_{m=1}^{M} (-1)^m A_m k^m = 1 + \sum_{m=1}^{M} A_m k^m \tag{31}$$

from which the A_m are evaluated by choosing M different values $S_\ell(k_i)$. The poles a_i are then determined as the zeros of the polynomial in the denominator of Eq. (30).

Once the a_i are found, one has to extract the α's and β's and their distribution on the k–plane. In the absence of bound states we have

$$\begin{aligned} N_\xi &= N_\sigma \\ M &= N_\sigma + N_\xi \\ N_\tau &= 0 \end{aligned}$$

from which

$$N_\xi = N_\sigma = \frac{M}{2} \tag{32}$$

In practice one varies M and the position k_i until a good fitting of $S_\ell(k)$ at all energies is achieved that fulfills the condition (32). In the presence of bound states the sorting is quite tricky. For example, in the presence of one bound state one has

$$\begin{aligned} N_\xi &= N_\sigma \\ M &= N_\sigma + N_\xi \\ N_\tau &= 1 \end{aligned}$$

Thus

$$N_\xi = \frac{M}{2}\,, \qquad N_\sigma = \frac{M-2}{2}\,, \qquad N_\tau = 1\,. \tag{33}$$

The number of poles in the upper k–plane N_u is given by

$$N_u = N_\xi + N_\tau = \frac{M}{2} + 1$$

while the number of poles in the lower k–plane N_l by

$$N_l = N_\sigma = \frac{M}{2} - 1\,.$$

Therefore

$$N_u = N_l + 2\,.$$

The same argumentation can be used for any number of bound states N_τ to obtain

$$N_u = N_l + 2N_\tau\,.$$

This condition must be satisfied for a correct construction of a potential.

Table 1: Comparison of the parameters of the first resonances generated in each partial wave by the exact potential (19) and by the approximate analytical form (20).

	exact potential		fitted potential	
ℓ	E_r (MeV)	Γ (MeV)	E_r (MeV)	Γ (MeV)
0	2.252380731	0.000118256	2.2520	0.0001179
1	0.807634844	0.000000110	0.8082	0.000000110
2	2.384151637	0.000082862	2.3843	0.000082812
3	1.009031953	0.000000046	1.0095	0.000000046
4	2.676524768	0.000027824	2.6768	0.00002783

Table 2: Spectral points generated by the $\alpha - \alpha$ potential proposed by Buck *et al.* [23].

	momentum (fm^{-1})		energy (MeV)	
ℓ	$\mathrm{Re}\,(k)$	$\mathrm{Im}\,(k)$	$\mathrm{Re}\,(E)$	Γ
0	0	2.63671	−72.62600	0
0	0	1.56602	−25.61905	0
2	0	1.45123	−22.00095	0
0	0.13098	−0.00017340	0.17922	0.00094905
2	0.53895	−0.061203	2.99519	1.37832
4	1.07513	−0.084009	12.00121	3.77407
6	1.85894	−0.48994	33.59171	38.05717

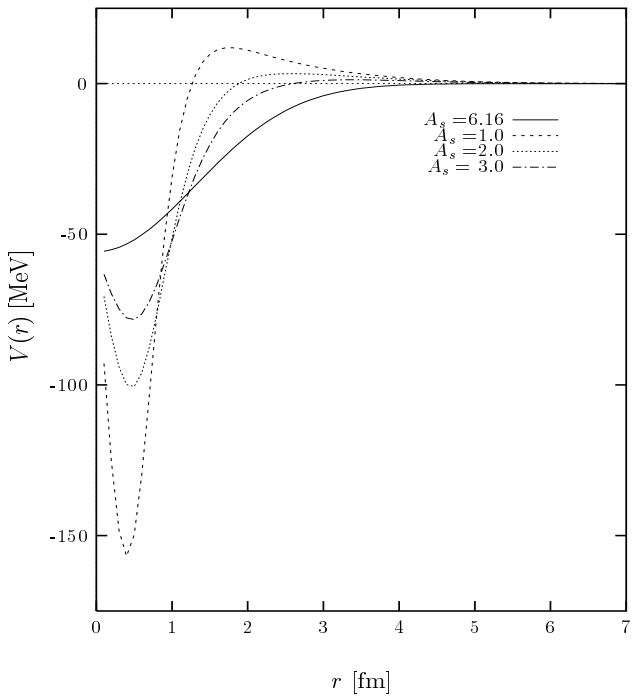

Figure 1: Bound state and phase equivalant potentials for the nucleon–α interaction. These potentials generate different resonance spectra.

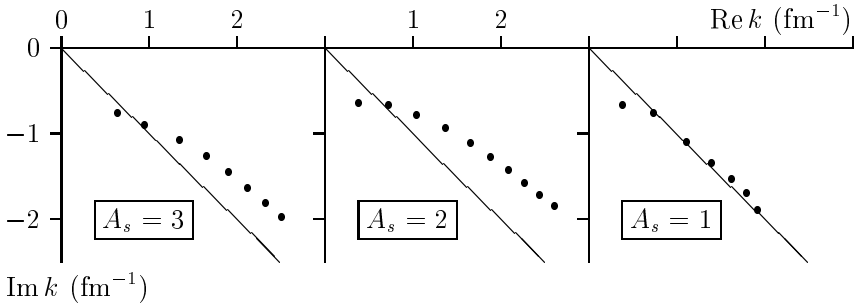

Figure 2: Distribution of the Jost function zeros (filled circles) in the complex k–plane for the S–wave N–α potential for three different values of the asymptotic normalization constant A_s. The diagonal of the fourth quadrant represents the threshold boundary $\mathrm{Re}\, E = 0$.

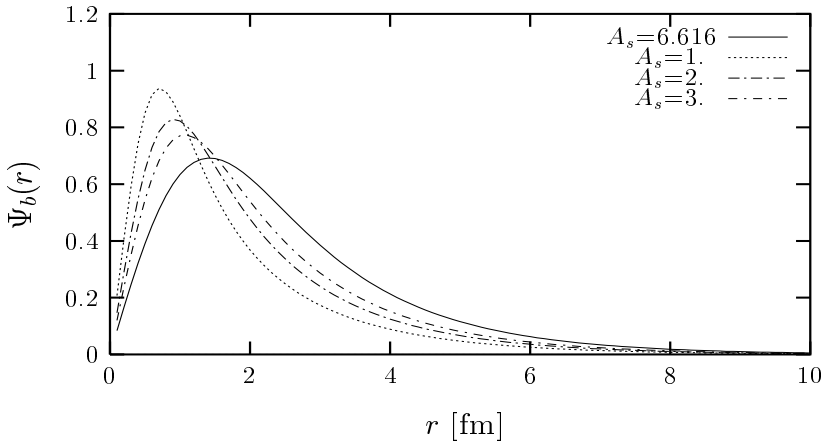

Figure 3: Bound state wave functions generated by the potentials of Fig. 1

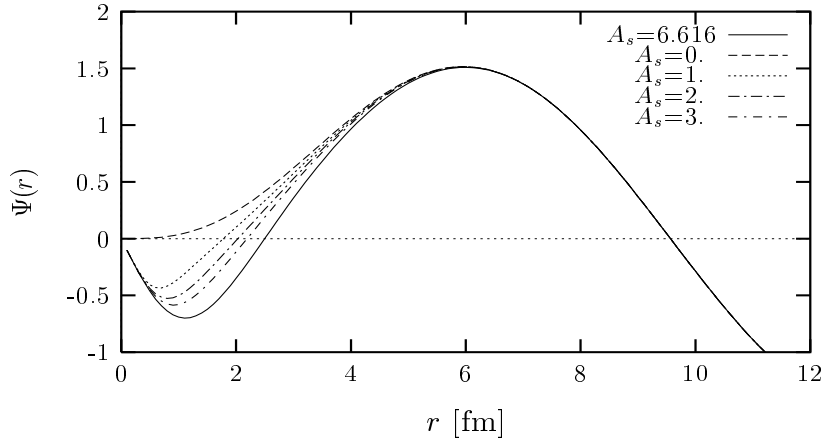

Figure 4: Scattering wave functions generated by the potentials of Fig. 1 for the center of mass energy $E = 5\,\mathrm{MeV}$. The $A_s = 0$ corresponds to the shallow $V^{(2)}$ potential that generates a nodeless wave function at short distances.